



CHORUS

This is the accepted manuscript made available via CHORUS. The article has been published as:

Vortex and Meissner phases of strongly interacting bosons on a two-leg ladder

M. Piraud, F. Heidrich-Meisner, I. P. McCulloch, S. Greschner, T. Vekua, and U. Schollwöck

Phys. Rev. B **91**, 140406 — Published 10 April 2015

DOI: [10.1103/PhysRevB.91.140406](https://doi.org/10.1103/PhysRevB.91.140406)

Vortex and Meissner phases of strongly-interacting bosons on a two-leg ladder

M. Piraud,¹ F. Heidrich-Meisner,¹ I. P. McCulloch,² S. Greschner,³ T. Vekua,³ and U. Schollwöck¹

¹*Department of Physics and Arnold Sommerfeld Center for Theoretical Physics,
Ludwig-Maximilians-Universität München, 80333 München, Germany*

²*Centre for Engineered Quantum Systems, The University of Queensland, Brisbane, QLD 4072, Australia*

³*Institut für Theoretische Physik, Leibniz Universität Hannover, 30167 Hannover, Germany*

(Dated: March 16, 2015)

We establish the phase diagram of the strongly-interacting Bose-Hubbard model defined on a two-leg ladder geometry in the presence of a homogeneous flux. Our work is motivated by a recent experiment [Atala et al., Nature Phys. **10**, 588 (2014)], which studied the same system, in the complementary regime of weak interactions. Based on extensive density matrix renormalization group simulations and a bosonization analysis, we fully explore the parameter space spanned by filling, inter-leg tunneling, and flux. As a main result, we demonstrate the existence of gapless and gapped Meissner and vortex phases, with the gapped states emerging in Mott-insulating regimes. We calculate experimentally accessible observables such as chiral currents and vortex patterns.

Introduction. The quantum states of interacting electrons in the presence of spin-orbit coupling and magnetic fields are attracting significant attention in condensed matter physics because of their connection to Quantum Hall physics [1], topological insulators [2–4] and the emergence of unusual excitations in low dimensions [5, 6]. Recent progress with quantum gas experiments has led to the realization of artificial gauge fields [7], both in the continuum [8–10] and for bosons in optical lattices [11–14], paving the way for future experiments on the interplay of interactions, dimensionality, and gauge fields in a systematic manner. This has motivated theoretical research into the physics of strongly interacting particles in the presence of abelian and non-abelian gauge fields and various questions such as the Quantum Hall effect with bosons [15–22], unusual quantum magnetism [23–26], and the emergence of topologically protected phases [27–29] have been addressed.

Given the complicated interplay between interactions, gauge fields and dimensionality, one often has to resort to mean-field approaches to build up intuition for the emergent phases, which should be complemented by reliable analytical and numerical results. In one dimension, both bosonization [30] and numerical techniques such as the density matrix renormalization group (DMRG) method [31–33] provide powerful tools to characterize the emergent quantum phases. Here we consider interacting bosons on a two-leg ladder in the presence of a homogeneous magnetic flux (see Fig. 1 for a sketch of the model and definitions of parameters). Such a system has been realized in a recent experiment with bosons in optical lattices [34], yet in the weakly-interacting regime of high densities per site. The existence of a transition between a phase with Meissner-like chiral currents and a vortex phase as a function of flux and rung tunneling strength has been demonstrated [34], reminiscent of the field-dependence of currents in type-II superconductors. Here we provide complementary insights into the emergent phases in the strongly-interacting case where, in par-

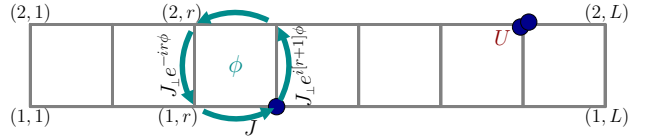


FIG. 1. (Color online) Sketch of the model Eq. (1): bosons on a two-leg ladder, with J and J_{\perp} the hopping matrix elements along the legs and rungs, respectively, with ϕ the magnetic flux per plaquette, and U the onsite interaction strength.

ticular, also Mott-insulating phases can appear [35, 36].

Bosons on a ladder subjected to gauge fields have been the topic of previous theoretical work [37–44] (see also [45, 46] for 2D lattices), yet complete quantitative phase diagrams are lacking. In our work, we use DMRG to systematically explore the full dependence on J_{\perp} , ϕ , and filling and, as a main result, we observe both gapped and gapless Meissner and vortex phases for strongly-interacting bosons. We focus on the gapped phases that emerge at a filling of one boson per rung, for which we present detailed results for chiral currents, the vortex density and current patterns in the vortex phase. In this Mott phase, Meissner currents are suppressed compared to superfluid phases, and can even decay to zero for an infinitely strong Hubbard interaction in the limit of large rung couplings $J_{\perp} \gg J$.

Hamiltonian and observables. The Hamiltonian is given by (see Fig. 1):

$$H = \sum_{\ell=1,2;r=1}^L \left[-J \left(a_{\ell,r+1}^{\dagger} a_{\ell,r} + \text{H.c.} \right) + \frac{U}{2} n_{\ell,r} (n_{\ell,r} - 1) \right] - J_{\perp} \sum_{r=1}^L \left(e^{-ir\phi} a_{1,r}^{\dagger} a_{2,r} + \text{H.c.} \right) \quad (1)$$

on a ladder with L rungs where $a_{\ell,r}^{\dagger}$ creates a boson on site $\ell = 1, 2$ of the r th rung. Energy is measured in units of J . We define the filling as $n = N/(2L)$, where N is the total number of bosons.

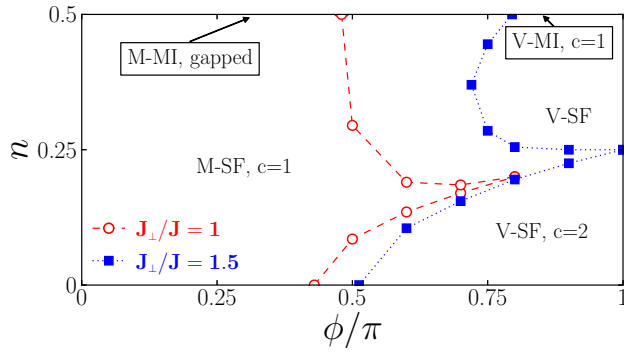


FIG. 2. (Color online) Phase diagram of HCBs for $J_{\perp}/J = 1$ (circles) and $J_{\perp}/J = 1.5$ (squares) as a function of flux ϕ and density n (DMRG data, $L = 101$). The region $0.5 < n \leq 1$ is related to the low-density regime by particle-hole symmetry.

On the one hand, the Hamiltonian (1) can be viewed as a minimal model for describing the edge states of a two-dimensional interacting Bose system pierced by a flux. On the other hand, we can interpret the system as a one-dimensional two-component gas [41, 42], where the two species are labeled with $\ell = 1, 2$. In the latter case, the term proportional to J_{\perp} breaks the $U(1)$ symmetry related to the conservation of the particle numbers of the individual components.

Local currents will be a key quantity for characterizing different phases. We define the currents along the legs $j_{\ell,r}^{\parallel}$ and rungs j_r^{\perp} as

$$j_{\ell,r}^{\parallel} = iJ \left(a_{\ell,r+1}^{\dagger} a_{\ell,r} - a_{\ell,r}^{\dagger} a_{\ell,r+1} \right) \quad (2)$$

$$j_r^{\perp} = iJ_{\perp} \left(e^{-ir\phi} a_{1,r}^{\dagger} a_{2,r} - e^{ir\phi} a_{2,r}^{\dagger} a_{1,r} \right). \quad (3)$$

The chiral (or Meissner) current is $j_c = \partial \mathcal{E}_0 / \partial \phi = \frac{1}{2L} |\sum_r \langle j_{1,r}^{\parallel} - j_{2,r}^{\parallel} \rangle|$, where \mathcal{E}_0 is the ground-state energy per site. Note that the operators given in Eqs. (2)-(3) depend on the gauge, but the associated expectation values are gauge invariant [46], as can be explicitly seen in the definition of the Meissner current. For the data shown in the figures, j_c is computed by restricting the sum to $r \in [-L/4, L/4]$ to suppress boundary effects, since in DMRG simulations we use open boundary conditions.

Phase diagram as a function of filling. Let us start by giving an account of our main results, which can be inferred from considering the limit of hard-core bosons (HCBs), i.e., $U/J = \infty$. Figure 2 shows the phase diagram for this case as a function of n and ϕ for $J_{\perp}/J = 1$ and 1.5. These results are based on a combination of a field-theory analysis and DMRG simulations for current correlation functions, the von Neumann entropy, excitation gaps, and the equation of state $n = n(\mu)$, where μ is the chemical potential.

In Fig. 2 we identify mainly four types of phases. At half-filling ($n = 0.5$), there is a Mott insulator (MI) with a mass gap for any value of ϕ and $J_{\perp} \neq 0$. At small values of ϕ , we find a Meissner phase (M-MI) while at large

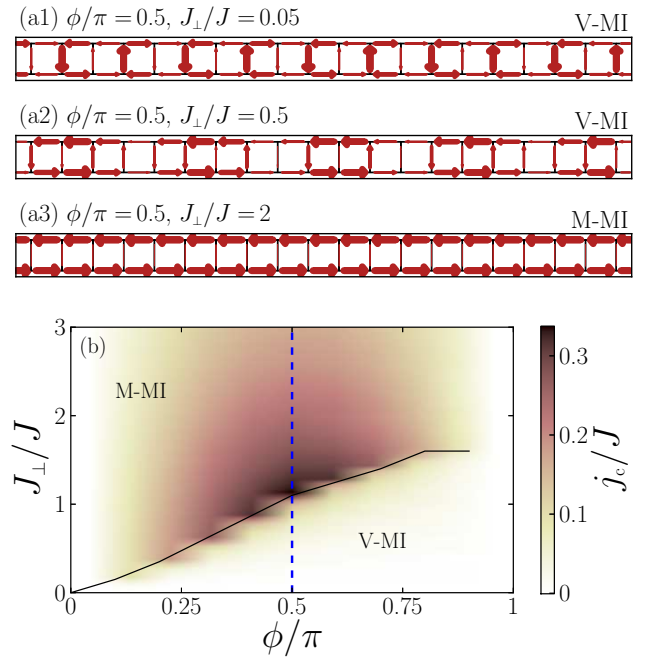


FIG. 3. (Color online) (a1)-(a3) Typical current patterns for $n = 0.5$, $\phi/\pi = 0.5$ and $J_{\perp}/J = 0.05, 0.5$ and 2 and (b) chiral current j_c as a function of ϕ and J_{\perp} (HCBs, $L = 101$). The width of the arrows in (a1)-(a3) is proportional to the expectation values of the local currents. In (b), the solid line locates the maximum at fixed ϕ and the dashed line the cut considered in Fig. 4.

ϕ , a gapless vortex state exists (V-MI). This confirms the prediction of a Mott gap for HCBs at $n = 0.5$ and $J_{\perp} \neq 0$ [35, 36] and the emergence of the Meissner currents and a vortex phase for $\phi \neq 0$ [41]. At finite values of $U/J < \infty$, there will be a MI-SF transition, with critical interaction strength depending on J_{\perp}/J [47]. At $n < 0.5$, there are superfluid phases which can again be divided into a Meissner superfluid (M-SF) and a vortex superfluid (V-SF). The terms Meissner and vortex state are justified by the existence of characteristic current patterns. Examples for $n = 0.5$ are shown in Figs. 3(a1)-(a2) (V-MI) and Fig. 3(a3) (M-MI) (current patterns in the M-SF and V-SF are qualitatively similar to the ones in the M-MI and V-MI, respectively: see Figs. S4(a)-(c) [47]). The Meissner phases have vanishing rung currents $\langle j_r^{\perp} \rangle$ but a finite chiral current j_c , while in the vortex phase, $\langle j_r^{\perp} \rangle \neq 0$ on finite systems, with various possible vortex patterns. The M-SF phase has one gapless mode (central charge $c = 1$), while the V-SF has $c = 2$. We expect M-SF and V-SF to be adiabatically connected to the corresponding phases established at weak interactions [34, 37, 44].

The M-SF phase penetrates into the V-SF phase at intermediate values of $J_{\perp} \sim J$. The vicinity of $\phi = \pi$ is special because at $n = 0.25$, a gapped charge-density-wave (CDW) phase emerges at $J_{\perp} \gtrsim 1.3J$. Once this happens, the M-SF phase touches this phase, splitting the V-SF into two lobes. Eventually, both the V-MI and

the upper lobe of the V-SF phase disappear for large $J_\perp \gtrsim 1.7J$. For $J_\perp \gtrsim 1.5J$, we find a jump in density at $\phi = \pi$, from $n > 0.25$ to the gapped $n = 0.5$ state, which for $J_\perp/J \rightarrow \infty$ extends down to $n = 0.25$.

Effective field theory. The nature of the phase transitions can be elucidated using bosonization. If we fix $J_\perp \neq 0$ and change the flux at half-filling, there is a commensurate-incommensurate (C-IC) quantum phase transition [30] from a gapped ($\phi < \phi^{\text{cr}}$) to a gapless ($\phi > \phi^{\text{cr}}$) behavior of the relative phase fluctuations of the two-leg system, whereas the total density mode is always gapped for strong interactions [47]. Away from $n = 0.5$, the total density mode becomes immediately gapless [36] and there is a C-IC transition in the relative degrees of freedom from a gapped to a gapless behavior as a function of flux [37]. This picture is confirmed by DMRG results for the von Neumann entropy (see Figs. S3 and S6 [47]) and consistent with the transitions shown in Fig. 2.

The emergence of a two-component Luttinger liquid (LL) at large values of ϕ becomes transparent in the low-density limit where it is connected with the development of a double-minimum structure in the single-particle dispersion ϵ_k for $\phi > \phi^{\text{cr}}(J_\perp)$ [42, 44]. Note that the physics at low densities is very similar to that of frustrated chains in high magnetic fields below saturation (see [54–56] and references therein). For bosons and in the limit of vanishing density, once the single-particle dispersion acquires a double-minimum, the $c = 2$ LL is stabilized. To show this, we solve the low-energy scattering problem of two bosons and extract the relevant scattering lengths. There are two important scattering processes at low energy: either the two bosons belong to the same minimum of ϵ_k (intra-species scattering) or they belong to different minima (inter-species scattering). In 1D, the scattering length is related to the scattering phase shift via $a_{i,j} = \lim_{K \rightarrow 0} [\cot(\delta_{i,j})/K]$, where K is the relative momentum of the two bosons and $i, j = 1, 2$ distinguish bosons belonging to the minimum in ϵ_k at $k < 0$ or $k > 0$, respectively. The scattering length is related to the amplitude of the contact potential of the two-component Bose gas $U_{i,j}(x - x') = g_{i,j}\delta(x - x')$ with $g_{i,j} = -2/(a_{i,j}m)$. By comparing the scattering lengths $a_{i,j}$ to each other we find that in strong coupling $a_{1,1} > a_{1,2}$, such that once the double-minimum structure appears in ϵ_k , the $c = 2$ LL is energetically preferred for $n \rightarrow 0$, consistently with the mean-field argument of [44] and with the DMRG results shown in Fig. 2.

Large J_\perp/J limit. Another interesting limit amenable to analytical treatment is the case of strong rung tunneling $J_\perp/J \rightarrow \infty$. In that regime we introduce a pseudo-spin-1/2 operator \vec{S}_r on each rung r associated to the states $(|1,0\rangle_r + e^{i\pi\phi}|0,1\rangle_r)/\sqrt{2} \rightarrow |\downarrow\rangle_r$, and $|0,0\rangle_r \rightarrow |\uparrow\rangle_r$. The effective spin-1/2 model for the

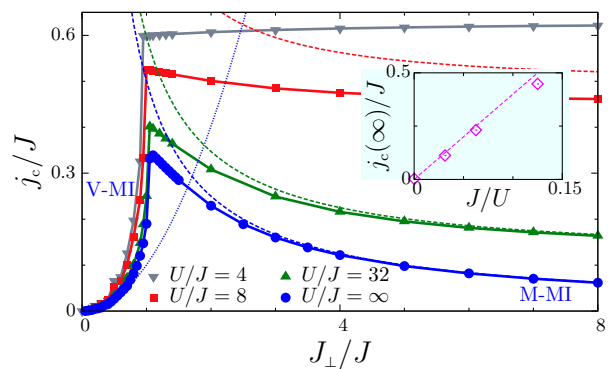


FIG. 4. (Color online) Cut through the phase diagram Fig. 3(b) at $\phi/\pi = 0.5$ for HCBs as well as $U/J = 4, 8, 16$ and 32 . Dashed lines: Theoretical predictions for $J_\perp \ll J$ and $J_\perp \gg J$ [see Eqs. (5) and (6)]. Inset: Asymptotic value $j_c(J_\perp/J \rightarrow \infty)$ as a function of $1/U$, together with $j_c(\infty) = 4J^2/U$. ($U/J < \infty$: $L = 60, L = 201$ for $U/J = \infty$).

special case of $\phi = \pi$ and to first order in J^2/J_\perp is [47]:

$$H_{\frac{1}{2}} = \frac{J^2}{2|J_\perp|} \sum_r \left(2S_r^z S_{r+1}^z - \left[S_r^+ \left(\frac{1}{2} - S_{r+1}^z \right) S_{r+2}^- + \text{h.c.} \right] \right). \quad (4)$$

In this basis, $n = 0.5$ corresponds to the fully polarized state $\prod_r |\downarrow\rangle_r$ and the vacuum of bosons $n = 0$ corresponds to $\prod_r |\uparrow\rangle_r$, while $n = 0.25$ implies a vanishing magnetization $\langle S_r^z \rangle$. The classical Néel-state $|\dots \uparrow \downarrow \uparrow \downarrow \dots\rangle$ is an eigenstate of the effective model Eq. (4) and for quarter-filling it becomes the ground state due to the dominant Ising interaction. Hence, in the vicinity of $\phi = \pi$ the ground state of bosons for $J_\perp/J \gg 1$ at quarter-filling ($n = 0.25$) is a doubly-degenerate CDW state, which breaks translational invariance. Away from $\phi \sim \pi$, the effective model undergoes a Kosterlitz-Thouless T transition at some $\phi_{\text{CDW}}^{\text{cr}}$ from the Néel state ($\phi_{\text{CDW}}^{\text{cr}} < \phi \leq \pi$) into a gapless XY phase ($\phi \leq \phi_{\text{CDW}}^{\text{cr}}$), the latter being characterized by $c = 1$. The existence of a fully gapped CDW state at $n = 0.25$ for strong J_\perp/J in the vicinity of $\phi = \pi$ and of a direct transition from the fully gapped state to a $c = 1$ phase with decreasing ϕ explains the tendency of the M-SF to pierce the V-SF (see Fig. 2).

The effective spin- $\frac{1}{2}$ model Eq. (4) further unveils the presence of a metamagnetic behavior just below the saturation magnetization, corresponding to a jump in the density of bosons from $n = 0.25$ to $n = 0.5$ at $J_\perp/J \rightarrow \infty$. Due to the absence of spin-inversion symmetry in Eq. (4) there is no such jump from $n = 0.25$ to $n = 0$. For $J_\perp/J < \infty$, this metamagnetic behavior survives with a jump between some $n > 0.25$ to $n = 0.5$, which explains the numerical data shown in Figs. S1 and S2 [47].

Dependence of currents on ϕ and J_\perp . Figure 3(b) shows the chiral current as a function of ϕ and J_\perp/J for HCBs at $n = 0.5$. The chiral current takes a maximum at the transition from the V-MI to the M-MI. Using field

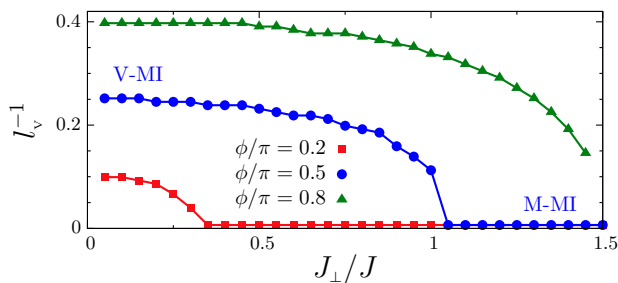


FIG. 5. (Color online) Vortex density l_v^{-1} , i.e., inverse typical extension l_v of the vortices (in lattice sites), versus J_\perp , for $\phi/\pi = 0.2, 0.5$ and 0.8 ($L = 101$).

theory, we derive an expression for the chiral current, in the regime $J_\perp \ll J$ and for small ϕ

$$j_c \sim \frac{J_\perp^2}{J\phi^{3-1/K_0}} + O(J_\perp^4), \quad (5)$$

where K_0 is the LL parameter for the Bose-Hubbard model of decoupled chains ($J_\perp = 0$), and ranges from $K_0 = \infty$, for $U = 0$, to $K_0 = 1$, for HCBs. The $j_c \propto J_\perp^2$ behavior is a generic result, valid for any repulsion U and filling [47]. Equation (5) implies that j_c increases the fastest with J_\perp at *small* values of ϕ . In particular, for HCBs, we obtain $j_c \sim (J_\perp/\phi)^2$.

For the opposite limit of large $J_\perp \gg J$, we use perturbation theory at $n = 0.5$ [47] to derive that for $U/J \gg 1$

$$j_c = \frac{J^2(4J_\perp + U)^2}{2J_\perp U(2J_\perp + U)} \sin(\phi). \quad (6)$$

Therefore, in the limit of infinitely strong interactions, the chiral current decays to zero in the M-MI as $j_c \propto 1/J_\perp$, contrary to the behavior at finite $U/J < \infty$ where the chiral current saturates at large $J_\perp \gg J$, as $j_c(\infty) \propto 1/U$ (see the inset in Fig. 4). This latter saturation is known from the $U = 0$ limit [34, 42] and is also observed in M-SF phases for $U \neq 0$ (results not shown).

Figure 4 presents a cut of Fig. 3 at $\phi = \pi/2$, together with finite U/J data. The analytical predictions for the weak- and strong-coupling regimes from Eqs. (5) and (6) agree very well with our DMRG data for $U/J \gg 1$ [dashed lines in Fig. 4]. The essential features of the HCB case carry over to finite values of $U/J < \infty$, yet a finite U suppresses the chiral current, which should be accessible in experiments.

The vortex phases can be further characterized by their current patterns which bear well-defined structures, with varying spatial extension and density as a function of J_\perp and ϕ . For the parameters of Fig. 3(a1), the sign of the current alternates along the legs, reminiscent of the chiral MI phase discussed in [39, 40]. These structures can be quantitatively studied by analyzing the rung currents $\langle j_r^\pm \rangle$. Figure 5 shows the vortex density l_v^{-1} at $n = 0.5$ as a function of J_\perp/J for various values of ϕ ,

where l_v is the typical size of vortices extracted from the Fourier transform of the real-space patterns $\langle j_r^\pm \rangle$ over $r \in [-L/4, L/4]$. This can be interpreted as a measure of the order parameter of the transition from the Meissner into the vortex phase [37]. As expected, l_v^{-1} decreases to zero as the transition into the M-MI phase is approached, where only longitudinal currents survive. This is consistent with field theory predictions, which also provide that in the $J_\perp \ll J\phi$ limit, $l_v^{-1} \sim \phi$ [47]. The rung-current correlation function $\langle j_r^\pm j_{r'}^\pm \rangle$ decays algebraically in all vortex phases (see Fig. S5 [47]), unlike in the so-called chiral MI phase [39, 40] realized for $U/J < \infty$, $\phi = \pi$, $J_\perp = J$, and $n = 1$, which has long-range rung-current correlations.

Summary. Based on a combined DMRG and field-theoretical study, we obtained the phase diagram of strongly interacting bosons on a two-leg ladder in the presence of a homogeneous flux per plaquette. We demonstrated the existence of both gapless and gapped Meissner and vortex phases, where the gapped Meissner phase emerges in the Mott-insulating regime. The chiral current is suppressed by interactions and for HCBs it decays to zero in the M-MI, with increasing J_\perp . These results substantially extend previous studies of related models [39–41] and confirm various predictions from field theory [37, 44]. We provided analytical results for the weak- and strong-coupling limit, in very good agreement with numerical data. Our findings will provide guidance for future experimental studies (similar to [34]) of the strongly-interacting regime. The interaction strength, density and the ratio of hopping matrix elements can routinely be tuned in optical lattice experiment [57], and so far, $\phi = \pi/2$ has been realized [13, 14, 34]. Interesting extensions of our present study include the current patterns in harmonic traps. For this case, our results for $n = n(\mu)$ provide information about the real-space density profiles via the local density approximation. Moreover, there is the possibility to stabilize vortex solids [37], which are so far elusive in the strongly-interacting regime at incommensurate fillings. In the strong-coupling limit $U \gg J$, vortex solids are not observed in our numerical data either in the superfluid or in the $n = 0.5$ Mott phase, as opposed to the $n = 1$ Mott phase for moderate values of U/J [39, 40], where a vortex solid appears at $\phi = \pi$.

Note added. Very recently, two more experimental studies have investigated fermions [58] and bosons [59] on ladders in optical lattices in the presence of artificial gauge fields.

We thank A. Paramekanti and I. Bloch for helpful discussions. The research of M.P. was supported by the European Union through the Marie-Curie grant 'ToPOL' (No. 624033) (funded within FP7-MC-IEF). This work was also supported in part by National Science Foundation Grant No. PHYS-1066293 and the hospitality of the Aspen Center for Physics. S.G. and T.V. are supported by the QUEST and DFG Research Training Group (Graduiertenkolleg) 1729, and I.M.C. acknowl-

edges funding from the Australian Research Council Centre of Excellence for Engineered Quantum Systems.

-
- [1] D. J. Thouless, M. Kohmoto, M. P. Nightingale, and M. den Nijs, *Phys. Rev. Lett.* **49**, 405 (1982).
- [2] C. L. Kane and E. J. Mele, *Phys. Rev. Lett.* **95**, 146802 (2005).
- [3] M. Z. Hasan and C. L. Kane, *Rev. Mod. Phys.* **82**, 3045 (2010).
- [4] X.-L. Qi and S.-C. Zhang, *Rev. Mod. Phys.* **83**, 1057 (2011).
- [5] A. Kitaev, “Unpaired majorana fermions in quantum wires,” (2000), arXiv:cond-mat/0010440.
- [6] L. Fu and C. L. Kane, *Phys. Rev. Lett.* **100**, 096407 (2008).
- [7] J. Dalibard, F. Gerbier, G. Juzeliūnas, and P. Öhberg, *Rev. Mod. Phys.* **83**, 1523 (2011).
- [8] Y.-J. Lin, R. L. Compton, K. Jiménez-García, J. V. Porto, and I. B. Spielman, *Nature (London)* **462**, 628 (2009).
- [9] Y.-J. Lin, R. L. Compton, Jiménez-García, W. D. Phillips, J. V. Porto, and I. B. Spielman, *Nature Phys.* **7**, 531 (2011).
- [10] K. Jiménez-García, L. J. LeBlanc, R. A. Williams, M. C. Beeler, A. R. Perry, and I. B. Spielman, *Phys. Rev. Lett.* **108**, 225303 (2012).
- [11] M. Aidelsburger, M. Atala, S. Nascimbène, S. Trotzky, Y.-A. Chen, and I. Bloch, *Phys. Rev. Lett.* **107**, 255301 (2011).
- [12] J. Struck, C. Ölschläger, M. Weinberg, P. Hauke, J. Simonet, A. Eckardt, M. Lewenstein, K. Sengstock, and P. Windpassinger, *Phys. Rev. Lett.* **108**, 225304 (2012).
- [13] M. Aidelsburger, M. Atala, M. Lohse, J. T. Barreiro, B. Paredes, and I. Bloch, *Phys. Rev. Lett.* **111**, 185301 (2013).
- [14] H. Miyake, G. A. Siviloglou, C. J. Kennedy, W. C. Burton, and W. Ketterle, *Phys. Rev. Lett.* **111**, 185302 (2013).
- [15] A. Sørensen, E. Demler, and M. Lukin, *Phys. Rev. Lett.* **94**, 086803 (2005).
- [16] R. Palmer and D. Jaksch, *Phys. Rev. Lett.* **96**, 180407 (2006).
- [17] M. Hafezi, A. Sørensen, E. Demler, and M. Lukin, *Phys. Rev. A* **76**, 023613 (2007).
- [18] N. R. Cooper, *Advances in Physics* **57**, 539 (2008).
- [19] A. Fetter, *Rev. Mod. Phys.* **81**, 647 (2009).
- [20] G. Möller and N. Cooper, *Phys. Rev. Lett.* **103**, 105303 (2009).
- [21] T. Senthil and M. Levin, *Phys. Rev. Lett.* **110**, 046801 (2013).
- [22] N. Regnault and T. Senthil, *Phys. Rev. B* **88**, 161106 (2013).
- [23] W. S. Cole, S. Zhang, A. Paramekanti, and N. Trivedi, *Phys. Rev. Lett.* **109**, 085302 (2012).
- [24] J. Radić, A. Di Ciolo, K. Sun, and V. Galitski, *Phys. Rev. Lett.* **109**, 085303 (2012).
- [25] Z. Cai, X. Zhou, and C. Wu, *Phys. Rev. A* **85**, 061605 (2012).
- [26] P. P. Orth, D. Cocks, S. Rachel, M. Buchhold, K. LeHur, and W. Hofstetter, *J. Phys. B: At. Mol. Opt. Phys.* **46**, 134004 (2012).
- [27] F. Grusdt, M. Hönig, and M. Fleischhauer, *Phys. Rev. Lett.* **110**, 260405 (2013).
- [28] F. Grusdt, F. Letscher, M. Hafezi, and M. Fleischhauer, *Phys. Rev. Lett.* **113**, 155301 (2014).
- [29] F. Grusdt and M. Hönig, *Phys. Rev. A* **90**, 053623 (2014).
- [30] T. Giamarchi, *Quantum Physics in One Dimension* (Clarendon Press, Oxford, 2004).
- [31] S. R. White, *Phys. Rev. Lett.* **69**, 2863 (1992).
- [32] U. Schollwöck, *Rev. Mod. Phys.* **77**, 259 (2005).
- [33] U. Schollwöck, *Ann. Phys. (NY)* **326**, 96 (2011).
- [34] M. Atala, M. Aidelsburger, M. Lohse, J. T. Barreiro, B. Paredes, and I. Bloch, *Nature Phys.* **10**, 588 (2014).
- [35] T. Vekua, G. Japaridze, and H.-J. Mikeska, *Phys. Rev. B* **67**, 064419 (2003).
- [36] F. Crépin, N. Laflorencie, G. Roux, and P. Simon, *Phys. Rev. B* **84**, 054517 (2011).
- [37] E. Orignac and T. Giamarchi, *Phys. Rev. B* **64**, 144515 (2001).
- [38] M.-C. Cha and J.-G. Shin, *Phys. Rev. A* **83**, 055602 (2011).
- [39] A. Dhar, M. Maji, T. Mishra, R. V. Pai, S. Mukerjee, and A. Paramekanti, *Phys. Rev. A* **85**, 041602 (2012).
- [40] A. Dhar, T. Mishra, M. Maji, R. V. Pai, S. Mukerjee, and A. Paramekanti, *Phys. Rev. B* **87**, 174501 (2013).
- [41] A. Petrescu and K. Le Hur, *Phys. Rev. Lett.* **111**, 150601 (2013).
- [42] D. Hügel and B. Paredes, *Phys. Rev. A* **89**, 023619 (2014).
- [43] R. Wei and E. J. Mueller, *Phys. Rev. A* **89**, 063617 (2014).
- [44] A. Tokuno and A. Georges, *New J. Phys.* **16**, 073005 (2014).
- [45] L.-K. Lim, C. Smith, and A. Hemmerich, *Phys. Rev. Lett.* **100**, 130402 (2008).
- [46] G. Möller and N. Cooper, *Phys. Rev. A* **82**, 063625 (2010).
- [47] See Supplemental Material [to be inserted], which includes Refs. [48–53].
- [48] T. Vekua, G. I. Japaridze, and H.-J. Mikeska, *Phys. Rev. B* **70**, 014425 (2004).
- [49] P. Fendley, H. Saleur, and A. B. Zamolodchikov, *Int. J. Mod. Phys. A* **8**, 5751 (1993).
- [50] A. B. Zamolodchikov, *Int. J. Mod. Phys. A* **8**, 1125 (1994).
- [51] K. Okunishi and T. Tonegawa, *Phys. Rev. B* **68**, 224422 (2003).
- [52] G. Vidal, J. I. Latorre, E. Rico, and A. Kitaev, *Phys. Rev. Lett.* **90**, 227902 (2003).
- [53] P. Calabrese and J. J. Cardy, *J. Stat. Mech.: Theory Exp.*, P06002 (2004).
- [54] M. Arlego, F. Heidrich-Meisner, A. Honecker, G. Rossini, and T. Vekua, *Phys. Rev. B* **84**, 224409 (2011).
- [55] A. K. Kolezhuk, F. Heidrich-Meisner, S. Greschner, and T. Vekua, *Phys. Rev. B* **85**, 064420 (2012).
- [56] I. T. Shyiko, I. P. McCulloch, J. V. Gumenjuk-Sichevska, and A. K. Kolezhuk, *Phys. Rev. B* **88**, 014403 (2013).
- [57] I. Bloch, J. Dalibard, and W. Zwerger, *Rev. Mod. Phys.* **80**, 885 (2008).
- [58] M. Mancini, G. Pagano, G. Cappellini, L. Livi, M. Rider, J. Catani, C. Sias, P. Zoller, M. Inguscio, M. Dalmonte, and L. Fallani, , arXiv:1502.02495 (unpublished).
- [59] B. K. Stuhl, H.-I. Lu, L. M. Ayccock, D. Genkina, and

I. B. Spielman, , arXiv:1502.02496 (unpublished).